Supplement of "The variation of particle number size distribution during the rainfall: wet scavenging and air masses changing"

Guangdong Niu[1], Ximeng Qi[1,2], Liangduo Chen[1], Lian Xue[1,2], Shiyi Lai[1], Xin Huang[1,2], Jiaping Wang[1,2], Xuguang Chi[1,2], Wei Nie[1,2], Veli-Matti Kerminen[3], Tuukka Petäjä[3], Markku Kulmala[3] and Aijun Ding[1,2]

[1]Joint International Research Laboratory of Atmospheric and Earth System Sciences, School of Atmospheric Sciences, Nanjing University, Nanjing, China.

[2]Jiangsu Provincial Collaborative Innovation Center for Climate Change, Nanjing University, Nanjing, China.

[3]Institute for Atmospheric and Earth Systems Research/Physics, Faculty of Science, University of Helsinki, Helsinki, Finland.

Correspondence to: Ximeng Qi (qiximeng@nju.edu.cn)

Contents of this file

Figures S1 to S14
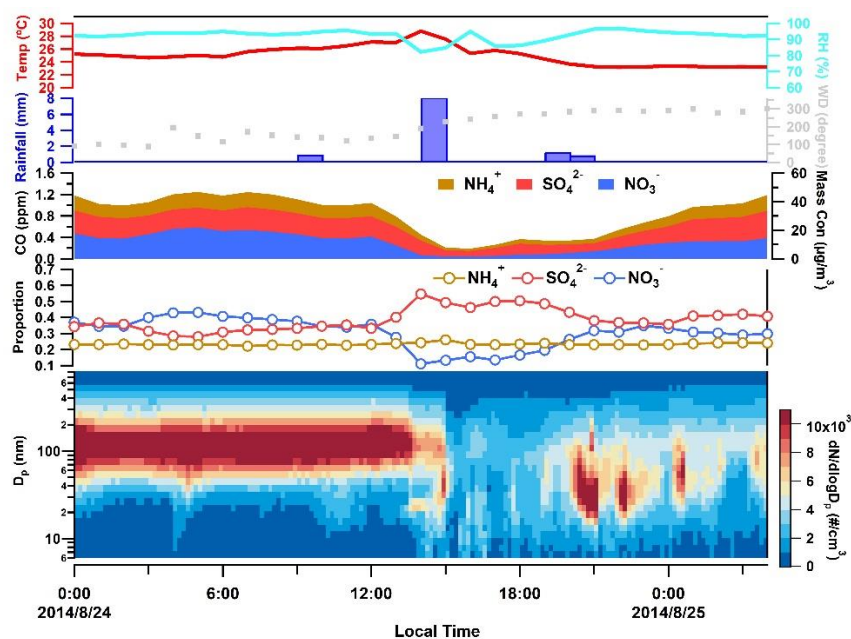
Figure S1. **Typical case for type i high BWSC event**. Top to bottom panels are time series of ambient temperature, RH, precipitation, wind direction, SNA (sulfate, nitrate, ammonium) concentrations, fractions of SNA in water soluble ions (WSIs), and particle number size distribution in Nanjing on 24-25 August 2014.

30
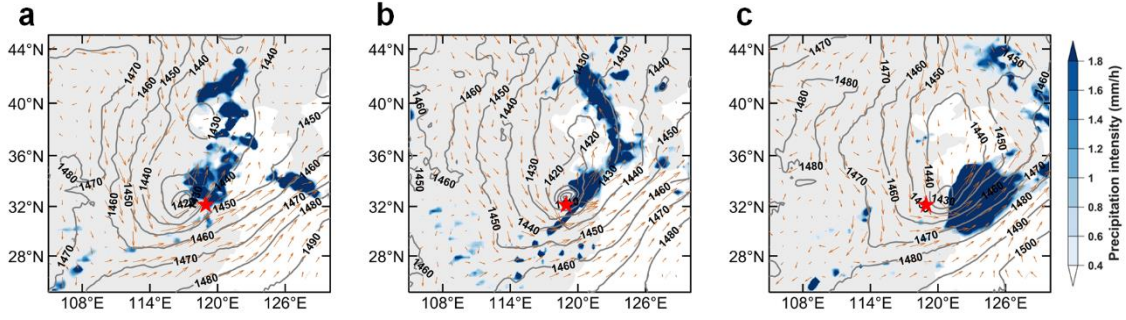
Figure S2. **Typical case for type i high BWSC event**. Distributions of winds and geopotential heights at 850 hPa and precipitation intensity (a) before, (b) at and (c) after the moment of sudden decrease in particle number concentration for the typical type i high BWSC event (24-25 August 2014) in Nanjing. The red pentagram shows the location of

35   SORPES station.
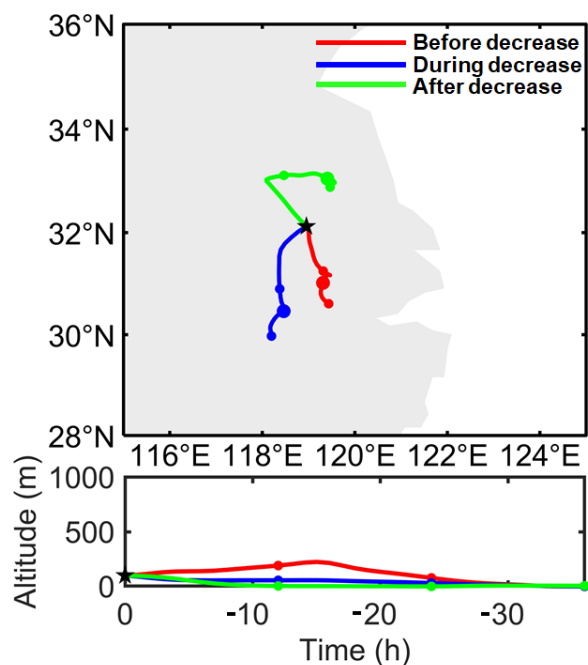
Figure S3. **Typical case for type i high BWSC event**. The backward trajectories of air masses before, at and after the moment of sudden decrease in particle number concentration for the typical type i high BWSC event (24-25 August 2014) in Nanjing. The black pentagram shows the location of SORPES station.

40
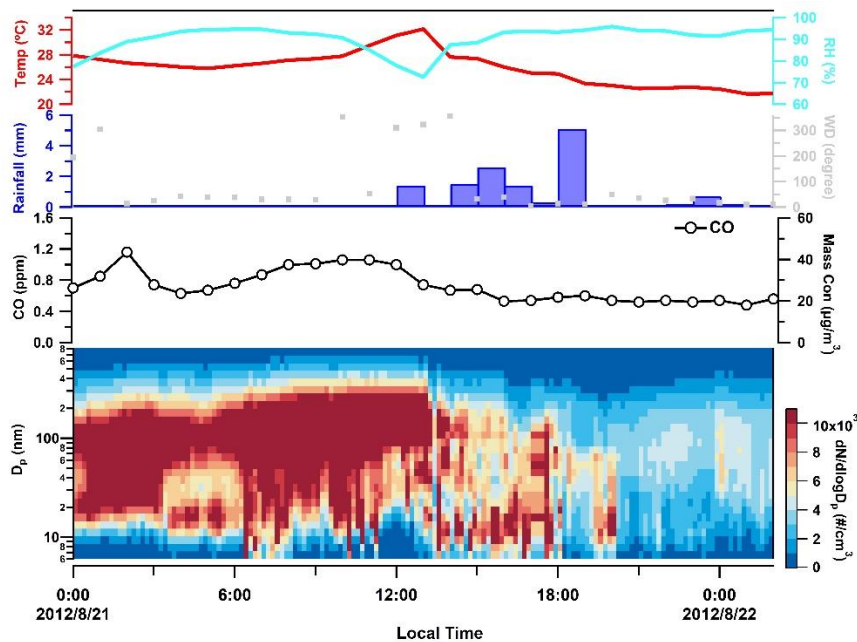
Figure S4. **Typical case for type ii high BWSC event**. Top to bottom panels are time series of ambient temperature, RH, precipitation, wind direction, CO concentration, and particle number size distribution in Nanjing on 21-22 August 2012.
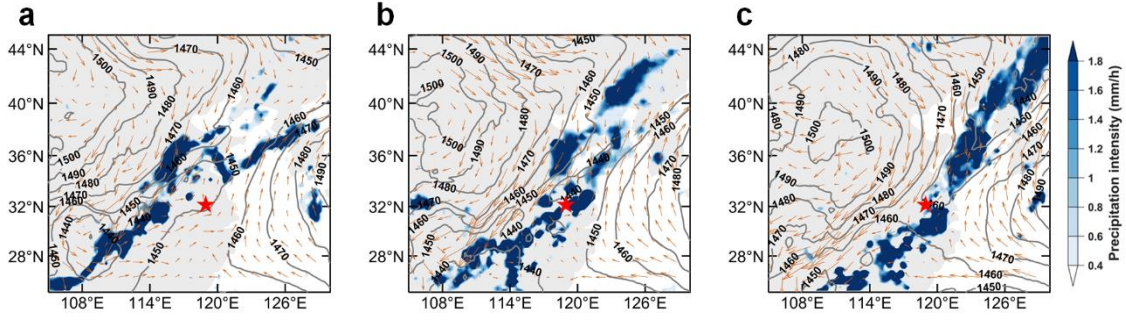
Figure S5. **Typical case for type ii high BWSC event.** Distributions of winds and geopotential heights at 850 hPa and precipitation intensity (a) before, (b) at and (c) after the moment of sudden decrease in particle number concentration for the typical type ii high BWSC event (21-22 August 2012) in Nanjing. The red pentagram shows the location of SORPES station.

55
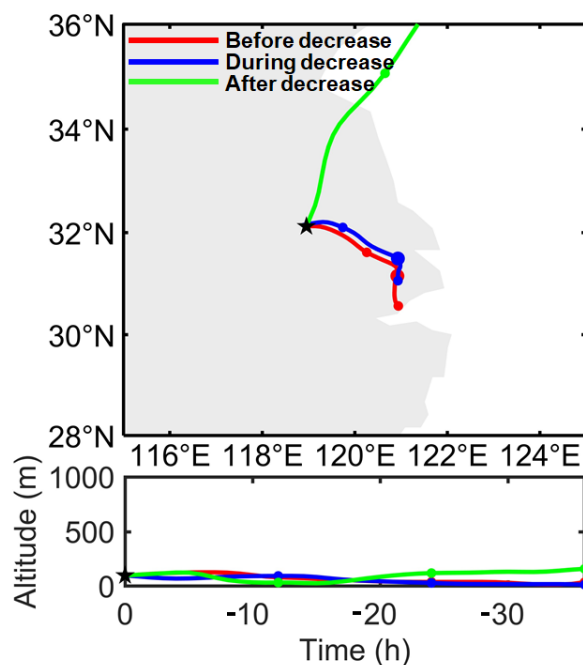
Figure S6. **Typical case for type ii high BWSC event**. The backward trajectories of air masses before, at and after the moment of sudden decrease in particle number concentration for the typical type ii high BWSC event (21-22 August 2012) in Nanjing. The black pentagram shows the location of SORPES station.
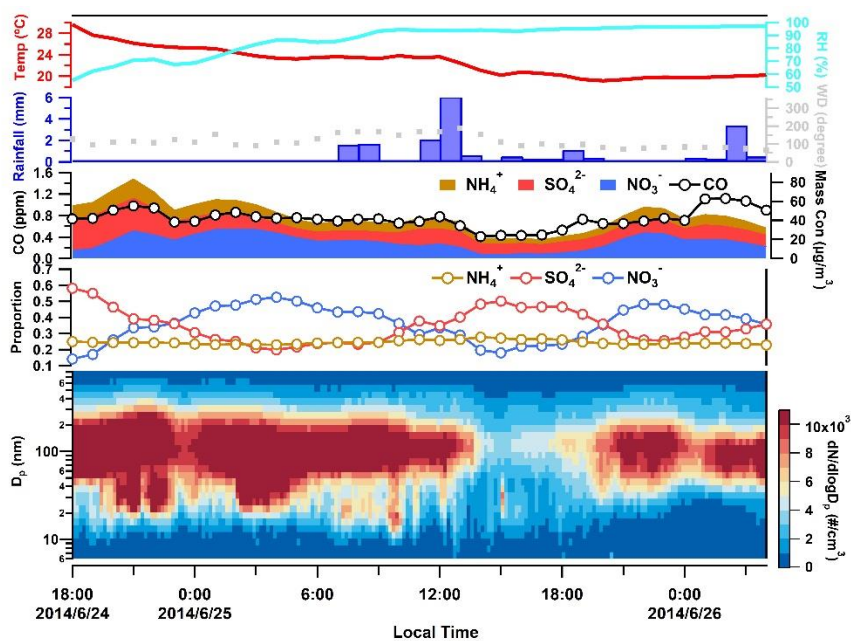
Figure S7. **Typical case for type iii high BWSC event**. Top to bottom panels are time series of ambient temperature, RH, precipitation, wind direction, CO concentration, SNA (sulfate, nitrate, ammonium) concentrations, fractions of SNA in WSIs, and particle number size distribution in Nanjing on 24-26 June 2014.
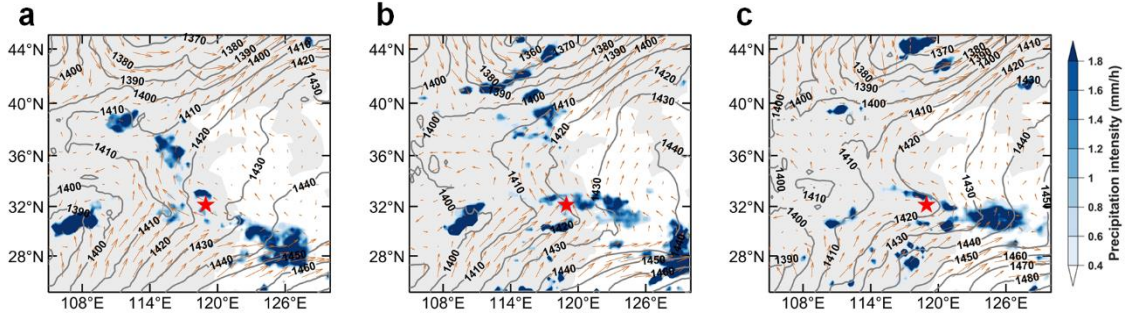
70 **Figure S8**. **Typical case for type iii high BWSC event.** Distributions of winds and geopotential heights at 850 hPa and precipitation intensity (a) before, (b) at and (c) after the moment of sudden decrease in particle number concentration for the typical type iii high BWSC event (24-26 June 2014) in Nanjing. The red pentagram shows the location of SORPES station.

75
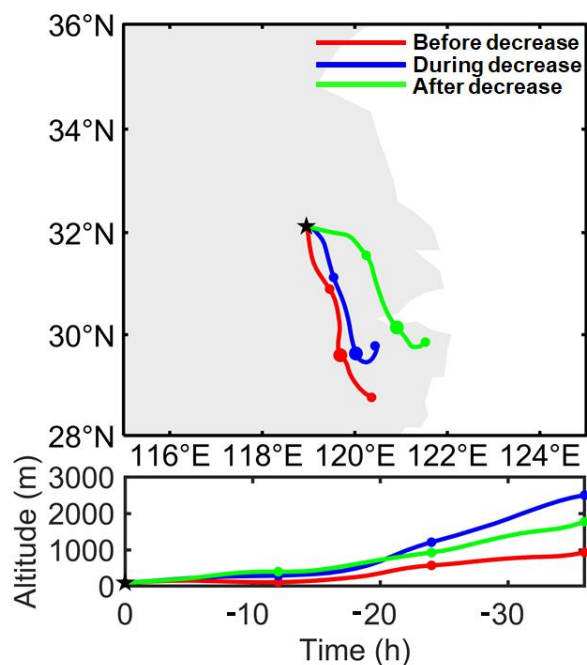
Figure S9. **Typical case for type iii high BWSC event.** The backward trajectories of air masses before, at and after the moment of sudden decrease in particle number concentration for the typical type iii high BWSC event (24-26 June 2014) in Nanjing. The black pentagram shows the location of SORPES station.
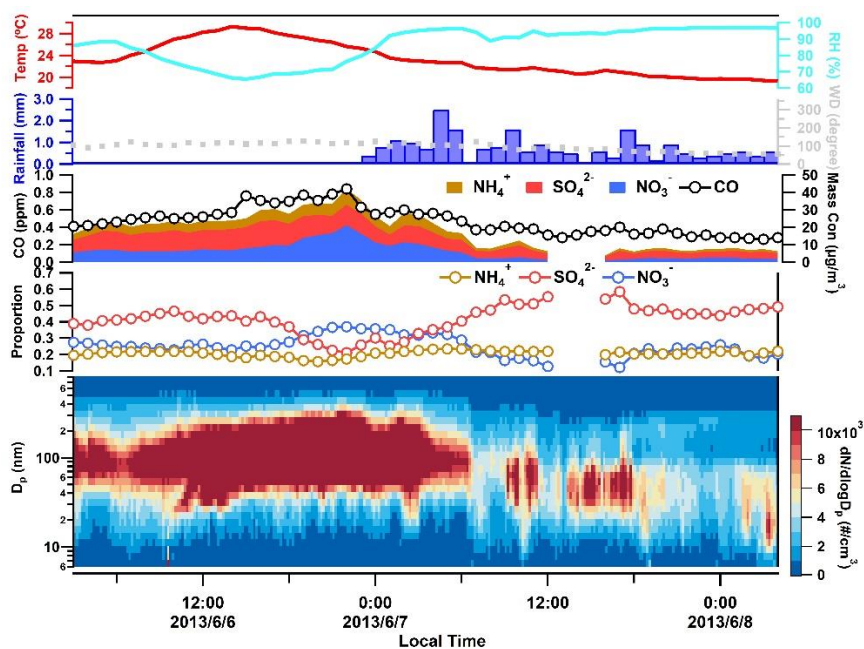
Figure S10. **Typical case for type iv high BWSC event**. Top to bottom panels are time series of ambient temperature, RH, precipitation, wind direction, CO concentration, SNA (sulfate, nitrate, ammonium) concentrations, fractions of SNA in WSIs, and particle number size distribution in Nanjing on 6-8 June 2013.
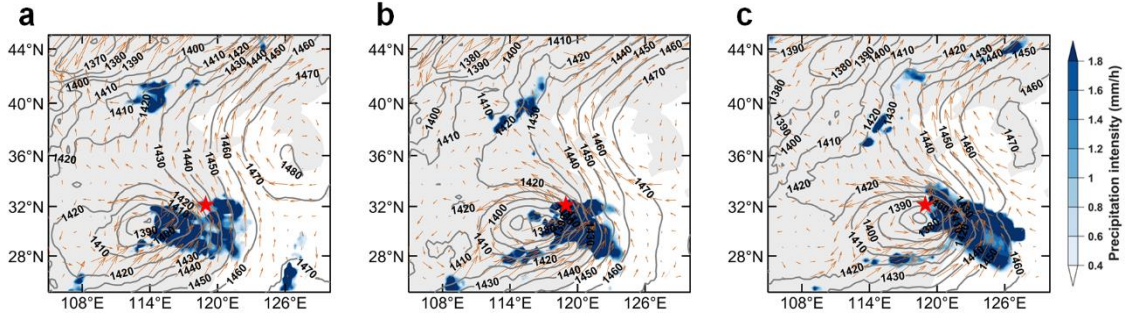
Figure S11. **Typical case for type iv high BWSC event**. Distributions of winds and geopotential heights at 850 hPa and precipitation intensity (a) before, (b) at and (c) after the moment of sudden decrease in particle number concentration for the typical type iv high BWSC event (6-8 June 2013) in Nanjing. The red pentagram shows the location of SORPES station.

95
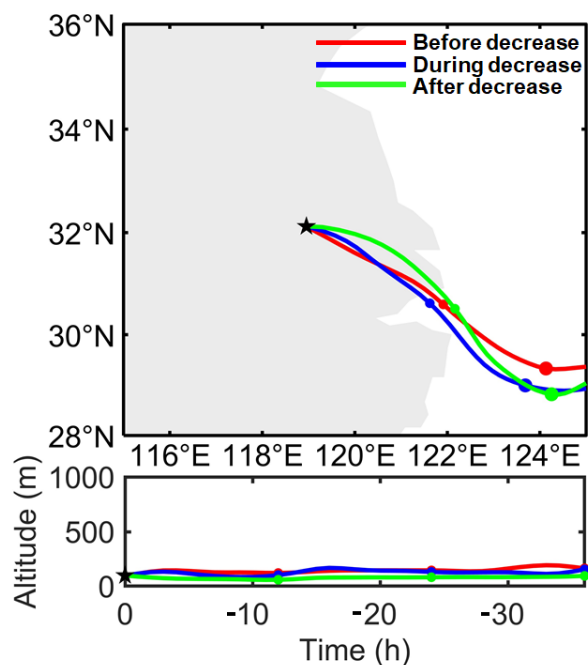
Figure S12. **Typical case for type iv high BWSC event.** The backward trajectories of air masses before, at and after the moment of sudden decrease in particle number concentration for the typical type iv high BWSC event (6-8 June 2013) in Nanjing. The black pentagram shows the location of SORPES station.
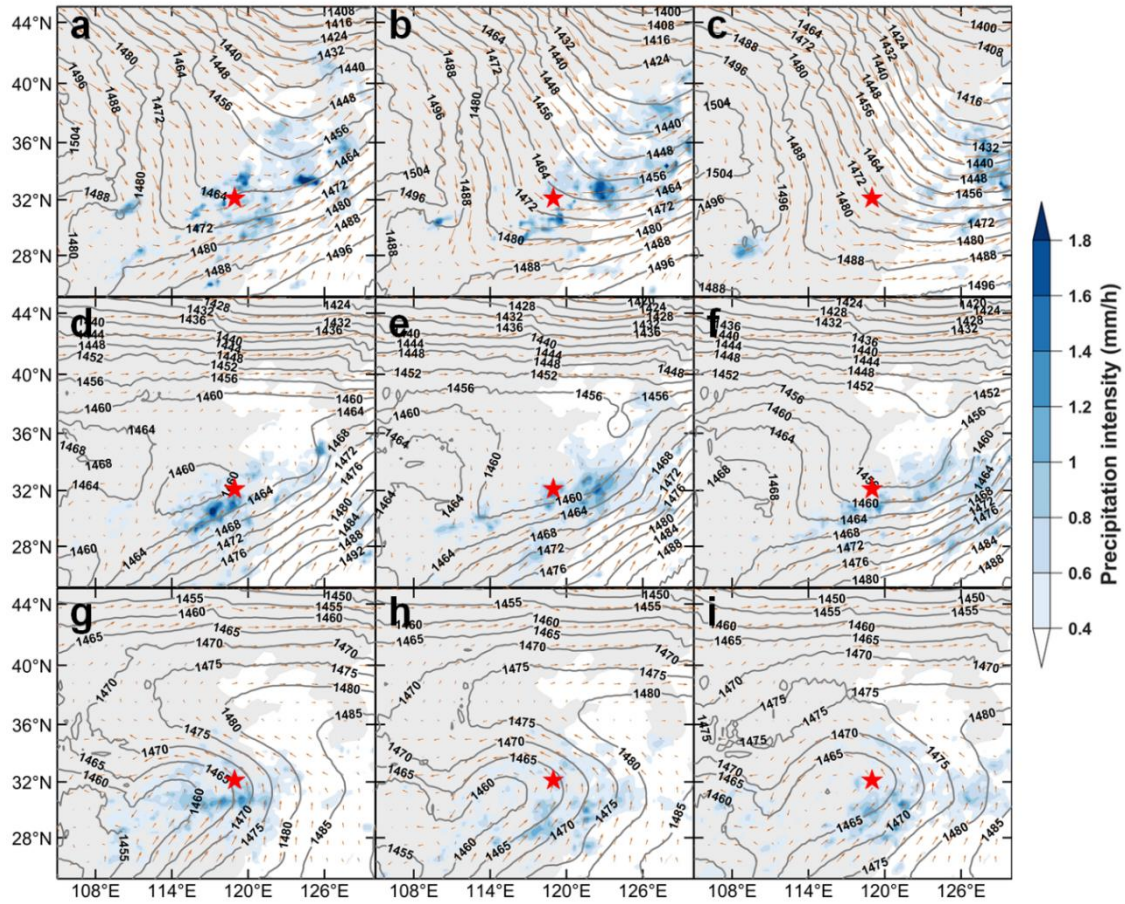
Figure S13. **Synoptic situations for normal scavenging events.** Distributions of winds and geopotential heights at 850 hPa and precipitation intensity before, during and after the rainfall events for (a-c) trough type, (d-f) vortex weakening type, and (g-i) vortex type of normal scavenging events. The red pentagram shows the location of SORPES station.
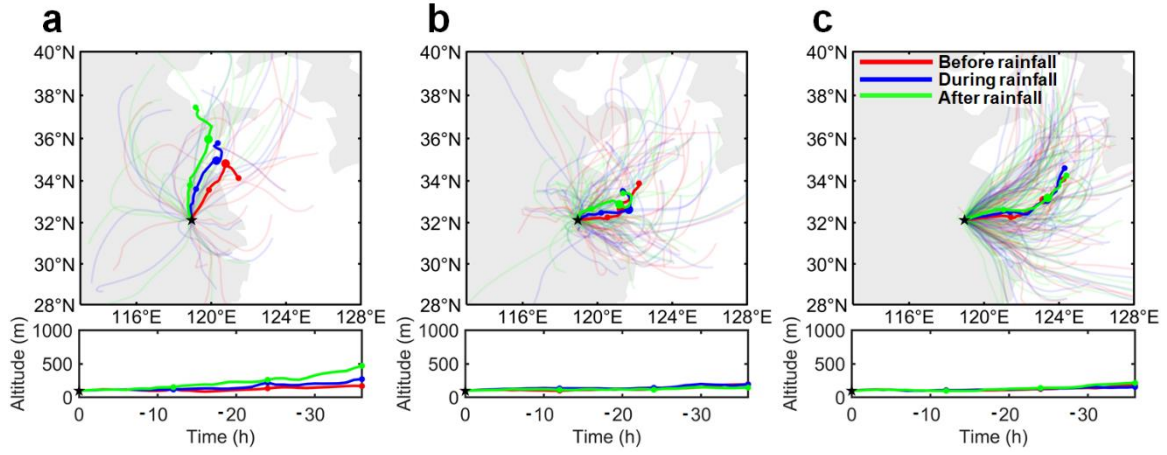
Figure S14. **Backward trajectories of air masses for normal scavenging events.** The backward trajectories of air masses before, during and after the rainfall events for (a) trough type, (b) vortex weakening type, and (c) vortex type of normal scavenging events. The black pentagram shows the location of SORPES station.